



The Inhibitive Effect of 2-Phenyl-3-nitroso-imidazo [1, 2-a]pyridine on the Corrosion of Steel in 0.5 M HCl Acid Solution

K. BOUHRIRA[#], F. OUAHIBA[§], D. ZEROUALI[#],
B. HAMMOUTI^{*§}, M. ZERTOUBI and N. BENCHAT[§]

[#]Laboratoire De Corrosion, Département Chimie
Faculté Des Sciences, Oran, Algérie

[§]LCAE-URAC18, Faculté des Sciences

Université Mohammed Premier, Oujda, Morocco

Laboratoire De Chimie Appliquée Et Environnement

Faculté Des Sciences, Ain Chock, Casa, Morocco

hammoutib@gmail.com

Received 18 December 2009; Accepted 10 February 2010

Abstract: The effect of 2-phenyl-3-nitroso-imidazo[1,2-a]pyridine (PNIP) on the corrosion inhibition of carbon-steel in 0.5 M HCl was studied by weight loss and different electrochemical techniques such as electrochemical impedance spectroscopy (EIS), potentiodynamic polarization. The obtained results showed that PNIP effectively reduces the corrosion rate of carbon steel. Inhibition efficiency (E%) increases with inhibitor concentration to attain 88% at 10⁻³ M. Adsorption of that PNIP on the carbon steel surface in 0.5 M HCl follows the Langmuir isotherm model. E% values obtained from various methods used are in good agreement. SEM characterization of the steel surface is made.

Keywords: Carbon steels, Corrosion Inhibitors, Polarization, Impedance, Adsorption.

Introduction

Mineral acid media are widely used for removal of undesirable scale and rust in many industrial processes such as pickling baths and surface treatment¹. To reduce metal lost as well as the consumption of acid, inhibitors are generally used. Heterocyclic inhibitors exhibit well through their heteroatoms and aromatic rings as well as double or triple bonds. Inhibitors act by adsorption to form a barrier between metal and acid ions²⁻⁵. This kind of organic molecules can adsorb on the metal surface because it can form a bond between the N electron pair and/or the π -electron cloud and the metal thereby reducing the corrosive attack on metals in acidic media.

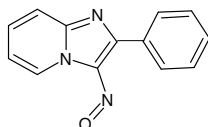
The existing data show that most organic inhibitors act by adsorption on the metal surface. This phenomenon is influenced by the nature and surface charge of metal, by the type of aggressive electrolyte and by the chemical structure of inhibitors^{6,7}. It is well known thatazole⁸⁻¹¹, imidazole¹²⁻¹⁵ and pyridine¹⁶⁻²¹ derivatives compounds are excellent inhibitors of corrosion for many metals and alloys in aggressive media.

The aim of this paper is to study the inhibiting action of a new pyridine compound (2-phenyl-3-nitroso-imidazo[1,2-a]pyridine). The electrochemical behaviour of steel in 0.5 M HCl media in the absence and presence of inhibitor have been studied by gravimetric method and electrochemical techniques such as potentiodynamic polarisation, linear polarisation and impedance spectroscopy (EIS). The scanning electron micrographs (SEM) of steel surface were taken in 0.5 M HCl with and without inhibitor.

Experimental

The organic compound tested as the corrosion inhibitor (2-phenyl-3-nitroso-imidazo[1,2-a]pyridine) was synthesized by Benchat *et al.*²², from 2-phenylimidazo[1,2-a]pyridine by using sodium nitrate in acetic acid at room temperature for one hours, the precipitate formed was filtered and then crystallized with ethanol gives 90% yield as green crystalline solid melting point 153-154 °C. The structure of 2-phenyl-3-nitroso-imidazo[1,2-a]pyridine was assigned on the basis of satisfactory analytical and spectroscopic data, MS (EI, *m/z*): 224 (M^+) / 100%; 194 ($M^+ - N=O$) / 35%; 147 ($M^+ - C_6H_5$) / 10%; 117 ($M^+ - [N=O] - [C_6H_5]$) / 12% , IR (KBr, cm^{-1}): 1580 (N=O) and the ¹H NMR, ¹³C NMR spectra taken in CDCl₃ for this compounds confirm this structure:

¹H NMR (CDCl₃, 300 MHz), δ : 10.00 – 9.97 (dd, 1H, $J_{H_5-H_6} = 6.60$ Hz, $J_{H_5-H_7} = 2.10$ Hz, H₅) ; 8.94 – 8.91 (dd, 1H, $J_{H_7-H_6} = 4.50$ Hz, $J_{H_7-H_5} = 2.10$ Hz, H₇) ; 8.77 – 8.75 (dd, 1H, $J_{H_6-H_5} = 6.90$ Hz, $J_{H_5-H_7} = 1.50$ Hz, H₆); 7.63 – 7.51 (m, 4H, H₁₀, H₁₁, H₁₃, H₁₄); 7.30 – 7.27 (dd, 1H, $J_{H_{12}-H_{11}} = 6.60$ Hz, $J_{H_{12}-H_{10}} = 4.50$ Hz, H₁₂); ¹³C NMR (CDCl₃, 75 MHz), δ : 158.8 (C_{8a}); 134.1 (C₃); 132.8 (C₅); 131.8 (C₇); 131.4 (C₂); 129.4 (C₆); 115.7 (C Ph). The molecular structure of the newly studied inhibitor is shown in Scheme 1.



Scheme 1. Chemical formula of 2-phenyl-3-nitroso-imidazo[1,2-a]pyridine

Gravimetric, Rp, polarisation and EIS measurements

The aggressive solution (0.5 M HCl) was prepared by dilution of analytical grade 37% HCl with double-distilled water. Prior to all measurements, the steel samples (0.159% C, 0.0173% Si; 0.376% Mn; 0.00305% P; 0.0791% Al; 0.00607% Cr; 0.0073% S, 0.0165% Cu, 0.00151% Ti, 0.00475% V, 0.0011% Sn, 0.00198% Ni and 99.33% Fe) were polished with different emery paper up to 1200 grade, washed thoroughly with double-distilled water, degreased with AR grade ethanol, acetone and drying at room temperature.

Gravimetric measurements were carried out in a double walled glass cell. The solution volume was 100 mL. The steel specimens used had a rectangular form (2 cm x 2 cm x 0.05 cm). The immersion time for the weight loss was 6 h at 308 K. After the corrosion test, the specimens of steel were carefully washed in double-distilled water, dried and then weighed. Duplicate experiments were performed in each case and the mean value of the weight loss is reported. Weight loss allowed us to calculate the mean corrosion rate as expressed in $mg.cm^{-2} h^{-1}$.

Electrochemical measurements were carried out in a conventional three electrode electrolysis Pyrex glass cell. The working electrode (WE) in the form of disc cut from steel has a geometric area of 1 cm². A saturated Ag/AgCl electrode and a disc platinum electrode were used respectively as reference and auxiliary electrodes, respectively. The temperature was thermostatically controlled at 298 ± 1 K.

Running on an IBM compatible personal computer, the Software Voltmaster 4 communicates with potentiostat (PGP 304), at a scan rate of 0.5 mV/sec. Before recording the polarisation curves, the steel electrode is polarised at -800 mV for 10 min. The potential of the electrode is swept to more positive values. The test solution is deaerated with pure nitrogen. Gas bubbling is maintained through the experiments.

Near E_{corr}, a scan through a potential range performs polarisation resistance (R_p) measurements. The potential range is ±10 mV around E_{corr}. The resulting current is plotted *versus* potential. R_p values are obtained from the current potential plot. The scan rate was 1 mV/sec.

The electrochemical impedance spectroscopy (EIS) measurements were carried out with the electrochemical system which included a digital potentiostat model Volta lab PGZ 100 computer at E_{corr} after immersion in solution without bubbling. After the determination of steady-state current at a given potential, sine wave voltage (10 mV) peak to peak, at frequencies between 100 kHz and 10 mHz were superimposed on the rest potential. Computer programs automatically controlled the measurements performed at rest potentials after 30 min of exposure. The impedance diagrams are given in the Nyquist representation.

Results and Discussion

Weight loss tests

Values of corrosion rates were determined after 6 h of immersion of steel in 0.5 M HCl at various concentrations of PNIP at 298 K and inhibition efficiencies are given in Table 1. The inhibition efficiency (E_w %) is determined by the following relation:

$$E_w \% = \frac{W_{\text{corr}} - W_{\text{corr}(\text{inh})}}{W_{\text{corr}}} \times 100 \quad (1)$$

Where W_{corr} and W_{corr (inh)} are the corrosion rates of steel with and without inhibitor, respectively.

Table 1 Gravimetric results of steel in acid without and with addition of PNIP

Concentration, M	W, mg/cm ² .h	E _w , %
0	1.725	-
5×10 ⁻⁵	0.909	47.3
10 ⁻⁴	0.787	54.4
5×10 ⁻⁵	0.321	79.6
10 ⁻³	0.286	83.4

Polarisation measurements

Current-potential characteristics resulting from polarisation curves of steel in 0.5 M HCl at various concentrations of the tested PNIP are shown in Figure 1. Table 2 collects the corrosion kinetic parameters such as E_{corr}, I_{corr} and β_c obtained from potentiodynamic polarization curves for steel in acid containing different concentrations of PNIP. In the case of polarization method the relation determines the inhibition efficiency (E_i %):

$$Ei \% = \frac{I_{\text{corr}} - I_{\text{corr(inh)}}}{I_{\text{corr}}} \times 100 \quad (2)$$

Where I_{corr} and $I_{\text{corr(inh)}}$ are the corrosion current density values without and with the inhibitor, respectively, determined by extrapolation of cathodic Tafel lines to the corrosion potential.

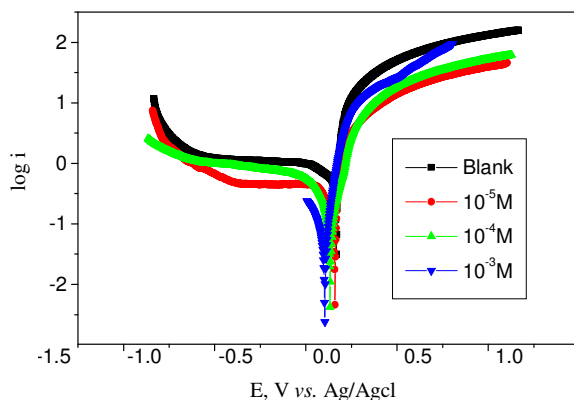


Figure 1. Polarization curves of steel at various concentrations of PNIP in 0.5 M HCl

Table 2. Corrosion parameters of steel at various concentrations of PNIP and corresponding inhibition efficiencies

C, M	E_{corr} , mV	I_{corr} , $\mu\text{A}/\text{cm}^2$	R_p , $\Omega.\text{cm}^2$	E%
0	-334	506.8	40.5	-
10^{-5}	-342	102.3	131.6	79.8
10^{-4}	-367	82.1	158.5	83.8
10^{-3}	-397	59.2	277.9	88.3

According to the results presented by Table 2, one notices that for this steel, the effectiveness of the inhibitor increases with the increase in the concentration of the inhibitor to reach a maximum of 88.3% for the concentration of 10^{-3} M, marked thus by a low density of the current of corrosion about $59.2 \mu\text{A}/\text{cm}^2$, is an increase in resistance to polarization R_p , the examination of the curves presented in Figure 2 shows that the anodic part, as of the these curves, is marked by stages, probably of the diffusion of oxygen, the anodic branches have the same pace relatively.

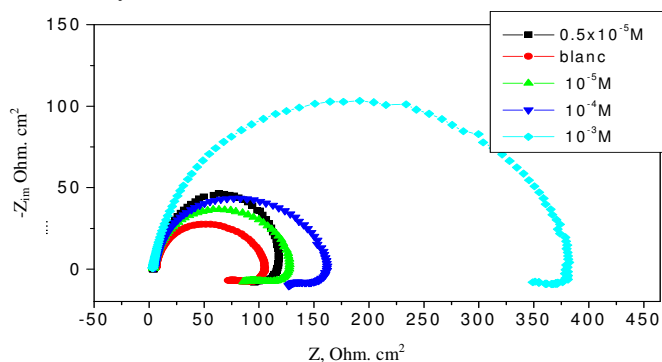


Figure 2. Nyquist diagram of C-steel in medium 0.5 M HCl at various concentrations of PNIP

The displacement of the potential of corrosion towards the cathodic values after the introduction of the inhibitor highlights the cathodic character of this latter. The functional atoms of the organic compound have a tendency to adsorb on metal surface²³. To show the major role of N atom in adsorption, Zucch *et al*²⁴. studied the influence of some compounds containing several nitrogen atoms on the corrosion of steel in the hydrochloric acid. The studied substances showed good inhibiting effectiveness (80-90%)²⁴.

The corresponding polarisation resistance (R_p) values of steel in 0.5 M HCl at different concentrations of PNIP are given in Table 2. The inhibition efficiency (E_{Rp}) was obtained by:

$$E_{Rp} \% = \frac{R'_p - R_p}{R'_p} \times 100 \quad (3)$$

R_p and R'_p are the polarisation resistance in absence and in presence of the inhibitor, respectively. It is evident that R_p increases with the inhibitor content indicating that PNIP opposed to the H^+ reduction.

Electrochemical impedance spectroscopy (EIS)

The corrosion behaviour of steel in hydrochloric acidic solution, in the absence and presence of PNIP, is also investigated by the electrochemical impedance spectroscopy (EIS) at 308 K after 30 min of immersion. The charge-transfer resistance (R_t) values are calculated from the difference in impedance at lower and higher frequencies. The double layer capacitance (C_{dl}) and the frequency at which the imaginary component of the impedance is maximal ($-Z_{max}$) are found as represented in equation:

$$C_{dl} = \frac{1}{\omega \cdot R_t} \quad \text{Where } \omega = 2\pi \cdot f_{max} \quad (4)$$

Impedance diagrams are obtained for frequency range 100 KHz - 10 mHz at the open circuit potential for steel in 1 M HCl in the presence and absence of PNIP. Nyquist plots for steel in 1 M HCl at various concentrations of PNIP are presented in Figure 3, the inhibition efficiency got from the charge-transfer resistance is calculated by the following relation:

$$E_{Rt} \% = \frac{R'_t - R_t}{R'_t} \times 100 \quad (5)$$

R_t and R'_t are the charge-transfer resistance values without and with inhibitor respectively. R_t is the diameter of the loop.

The examination of the results of Table 3 enables us to deduce the following points: Resistance from load transfer, R_o , increases with the concentration of the inhibitor, the values of R_t informs us about the kinetics of the reactions. R_t increases with the introduction of the inhibitor; this can be due to the blocking of the active sites by the film formed by the inhibitor at the surface of the metal while the capacity of the double layer decreases as the quantity of the inhibitor increases. The reduction in the capacity of the double layers is due to the adsorption of the inhibitor at the steel surface which causes the reduction of the active surface of the electrode. The inhibiting effectiveness increases with the concentration of the inhibitor to reach a maximum value from 73% to 10^{-3} M. The examination of the Figure 2 shows that, for all the concentrations used, the presence of only one capacitive loop at high frequencies and a second inductive loop which represents a modification of surface or a variation of the rates of covering, resulting from the phenomena of adsorption at low frequency²⁵. The improvement of resistance to corrosion could be allotted to the formation of a protective film; moreover, the capacities obtained are weaker than those generally allotted to the double layer ($50-200 \mu\text{f}/\text{cm}^2$)²⁶.

Table 3. Test results of impedance of C-steel in the medium 0.5 M HCl in the absence and the presence of the inhibitor at various concentrations

C, M	R_{es} , $\Omega \cdot \text{cm}^2$	R_t , $k\Omega \cdot \text{cm}^2$	C, $\mu\text{f}/\text{cm}^2$	E%
Blank	5.679	106.3	109.4	-
0.5×10^{-5}	3.839	122.5	49.06	13
10^{-5}	2.322	137.8	55.75	23
10^{-4}	1.624	162.1	34.93	46
10^{-3}	3.165	392.7	31.30	73

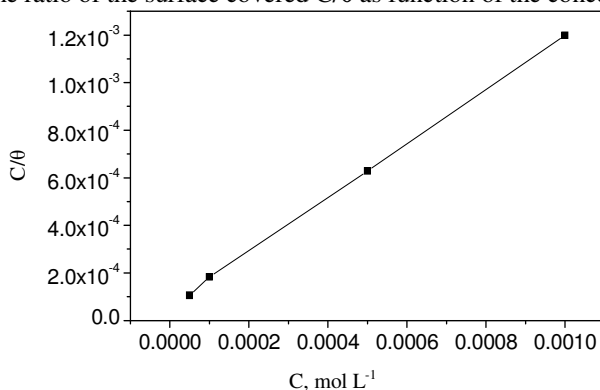
Adsorption isotherm

The Langmuir adsorption isotherm was found to be the best description of the adsorption behaviour of the tested inhibitor, which obeys to:

$$\frac{C_{\text{inh}}}{\theta} = \frac{1}{k} + C_{\text{inh}} \quad (6)$$

$$k = \frac{1}{55,5} \cdot \exp\left(-\frac{\Delta G_{\text{ads}}^{\circ}}{R \cdot T}\right) \quad (7)$$

C_{inh} is the inhibitor concentration; θ is the fraction of the surface covered, k is the adsorption coefficient and $\Delta G_{\text{ads}}^{\circ}$ is standard free energy of adsorption. Figure 3 shows the dependence of the ratio of the surface covered C/θ as function of the concentration (C) of PNIP.

**Figure 3.** Langmuir isotherm adsorption model of PNIP on the surface of steel in 0.5 M HCl

The obtained plot of inhibitor is linear with a slope 1.14 to close to unity. The regression coefficient is $R = 0.9998$. The intercept permit the calculation of the equilibrium constant $k = 17030.7 \text{ M}^{-1}$ which leads to evaluate $\Delta G_{\text{ads}}^{\circ} = -34.9 \text{ kJ/mol}$. The negative value of $\Delta G_{\text{ads}}^{\circ}$ indicates that the inhibitor is spontaneously adsorbed on the metal surface and shows also physical adsorption of PNIP²⁷.

MES

Figure 4 shows the scanning electron micrographs of steel after immersion for 6 h in 0.5 M HCl solution with and without PNIP. The specimen surface in Figure 4b appears to be roughened extensively by the corrosive environment and the porous layer of corrosion product is present. In presence of inhibitor, the data (Figure 4c) gave the surface of steel surface with absence of corrosion product. This may be interpreted by the adsorption of the inhibitor on the electrode surface.

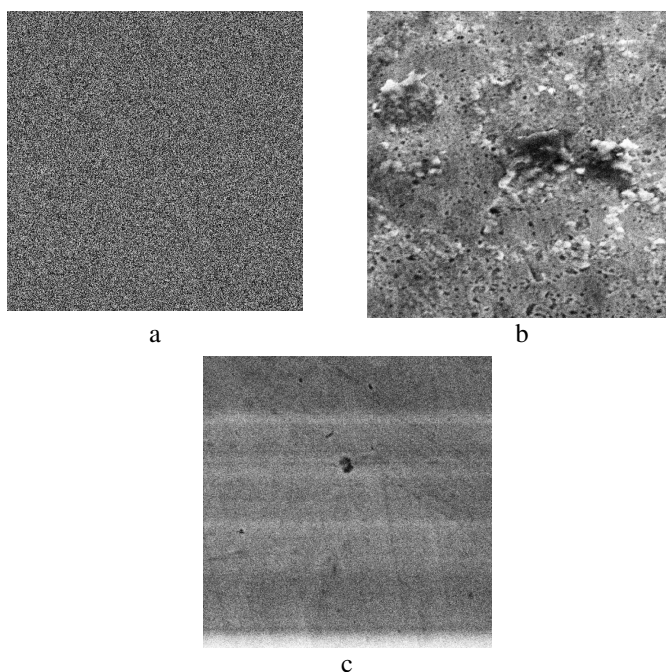


Figure 4. SEM of carbon steel: (a) steel polished; (b) steel immersed at 6 h in 0.5 M HCl; (c) steel immersed at 6 h in 0.5 M HCl + 0.5×10^{-3} M PNIP

Conclusion

The following main conclusions are drawn from this study:

- The protection efficiency increases with the increase of the inhibitor concentration.
- Polarization measurements show that the PNIP act a mixed inhibitor and the cathodic curves presented in the Tafel lines indicating that the hydrogen evolution reaction at the metal surface occurs through a pure mechanism of activation.
- PNIP adsorbs on the steel surface according to the Langmuir isotherm adsorption.
- SEM indicates the good inhibitory effect of studied PNIP.

References

1. Uhlig H H and Revie RW, Corrosion and Corrosion Control, Wiley, New York, 1985.
2. Saratha R and Vasudha V G, *E-J Chem.*, 2009, **6(4)**, 1003-1008.
3. Rafiquee M Z A, Khan S, Saxena N and Quraishi M A, *J Appl Electrochem.*, 2009, **39**, 1409-1417.
4. Khaled K F, Fadl-Allah S A and Hammouti B, *Mater Chem Phys.*, 2009, **117**, 148.
5. Bouklah M, Hammouti B, Lagrenée M and Bentiss F, *Corros Sci.*, 2006, **48**, 2831.
6. Upadhyay R K and Mathur S P, *E-J Chem.*, 2007, **4(3)**, 408-414.
7. Tebbji K, Hammouti B, Oudda H, Ramdani A and Benkadour M, *Appl Surf Sci.*, 2005, **252**, 1378.
8. Salghi R, Bazzi L, Hammouti B and Kertit S, *Bull Electrochem.*, 2000, **16**, 272.
9. Elouafi A, Hammouti, B, Oudda H, Kertit S, Touzani R and Ramdani A, *Anti-Corros Meth Mat.*, 2002, **49**, 199.

10. Bouklah N, Hammouti B, Benkaddour M, Attayibat A and Radi S, *Pigment Resin Technol.*, 2005, **34**, 197.
11. Touhami F, Aouniti A, Abed Y, Hammouti B, Kertit S, Ramdani A and Elkacemi K, *Corros Sci.*, 2000, **42**, 929.
12. Benabdellah M, Touzani R, Aouniti A, Dafali A, El Kadiri S, Hammouti B and Benkaddour M, *Mater Chem Phys.*, 2007, **105**, 373.
13. Tebbji K, Bouabdellah I, Aouniti A, Hammouti B, Oudda H, Benkaddour M and Ramdani A, *Mater Lett.*, 2007, **61**, 799.
14. Dafali A, Hammouti B, Aouniti A, Mokhlisse M, Kertit S and Elkacemi K, *Ann Chim Sci Matt.*, 2000, **25**, 437.
15. Dafali A, Hammouti B and Kertit S, *J Electrochem Soc India*, 2001, **50**, 62.
16. Tebbji K, Oudda H, Hammouti B, Benkaddour M, El Kodadi M and Ramdani A *Colloid Surf A: Physicochem Eng.*, 2005, **259**, 143.
17. Krim O, Elidrissi A, Hammouti B, Ouslim A and Benkaddour M, *Chem Eng Comm.*, 2009, **196**, 1536.
18. Hassan N and Holze R, *J Chem Sci.*, 2009, **121(5)**, 693-701.
19. Jamalizadeh E, Jafari AH and Hosseini SMA, *J Molecular Structure: Theochem*, 2008, **870**, 23.
20. Ergun U, Yüzer D and Emregül K C, *Materials Chemistry Physics*, 2008, **109**, 492.
21. Veloz M A and Martínez I G, *Corrosion*, 2006, **62**, 283
22. Benchat N, Abouricha S, Anafloos A, Mimouni M and Ben-Hadda T, El Bali B, Hakkou A and Hacht B, *Lett Drug Design Discovery*, 2004, **1**, 224-229.
23. Zhang D Q, Cai Q R, Gao L X and Lee K Y, *Corros Sci.*, 2008, **50**, 3615.
24. Zucch F and Trabanalli G, 7th Eur Symp Corrosion Inhibitors, Ann Univ Ferrera, Italy, 1990, 330.
25. Khaled K F, *Electrochem Acta.*, 2009, **54**, 4345.
26. Abed Y, Hammouti B, Touhami F, Aouniti A, Kertit S, Mansri A and Elkacemi K, *Bull Electrochem*, 2001, **17(3)**, 105-110.
27. Shamitha Begum A, Mallika A and Gayathri P, *E-J Chem.*, 2010, **7(1)**, 185-197.



Hindawi

Submit your manuscripts at
<http://www.hindawi.com>

